Geomechanics and Engineering, *Vol. 31, No. 5 (2022) 439-452*
https://doi.org/10.12989/gae.2022.31.5.439

Assessment of seismic stability of finite slope in c-ϕ soils - a plasticity approach

Shibsankar Nandi[1a], G. Santhoshkumar[2b] and Priyanka Ghosh*[1]

[1]*Department of Civil Engineering, Indian Institute of Technology Kanpur, Kanpur – 208 016, India*
[2]*School of Infrastructure, Indian Institute of Technology Bhubaneswar, Argul, Khordha, Odhisha – 752 050, India*

(*Received September 9, 2021, Revised August 26, 2022, Accepted September 25, 2022*)

Abstract. A forecast of slope behavior during catastrophic events, such as earthquakes is crucial to recognize the risk of slope failure. This paper endeavors to eliminate the significant supposition of predefined slip surfaces in the slope stability analysis, which questions the relevance of simple conventional methods under seismic conditions. To overcome such limitations, a methodology dependent on the slip line hypothesis, which permits an automatic generation of slip surfaces, is embraced to trace the extreme slope face under static and seismic conditions. The effect of earthquakes is considered using the pseudo-static approach. The current outcomes developed from a parametric study endorse a non-linear slope surface as the extreme profile, which is in accordance with the geomorphological aspect of slopes. The proposed methodology is compared with the finite element limit analysis to ensure credibility. Through the design charts obtained from the current investigation, the stability of slopes can be assessed under seismic conditions. It can be observed that the extreme slope profile demands a flat configuration to endure the condition of the limiting equilibrium at a higher level of seismicity. However, a concurrent enhancement in the shear strength of the slope medium suppresses this tendency by offering greater resistance to the seismic inertial forces induced in the medium. Unlike the traditional linear slopes, the extreme slope profiles mostly exhibit a steeper layout over a significant part of the slope height, thus ensuring a more optimized solution to the slope stability problem. Further, the susceptibility of the Longnan slope failure in the Huining-Wudu seismic belt is predicted using the current plasticity approach, which is found to be in close agreement with a case study reported in the literature. Finally, the concept of equivalent single or multi-tiered planar slopes is explored through an example problem, which exhibits the appropriateness of the proposed non-linear slope geometry under actual field conditions.

Keywords: earthquake; failure; numerical analyses; plasticity; slope stability

1. Introduction

These days, a few significant infrastructure projects are developed in sloping territories, where the ground profile is not traditionally plane. Natural slopes are generally found to be curvilinear following the geomorphological process to ensure the constant factor of safety along the slope face (Rieke-Zapp and Nearing 2005, Schor and Gray 2007, Utili and Nova 2007, Gray 2013, Jeldes *et al*. 2015). Regardless of whether they are natural or human-made structures, the stability analysis of slopes needs to be executed carefully (Wasowski *et al*. 2011). In general, the stability of slopes can be examined utilizing different hypotheses proposed by a few researchers (Fellenius 1936, Taylor 1937, Bishop 1955). However, these hypotheses are bound to static conditions.

A few studies (Ghanbari *et al*. 2013, Erzın and Cetin 2014, Terzi and Selcuk 2015, Nasiri *et al*. 2020) attempted to embrace the effect of earthquakes on slope stability analysis. During an earthquake event, the soil mass is exposed to horizontal and vertical shaking due to the propagation of seismic waves through the soil body. Propagation of such waves through the soil medium induces horizontal and vertical seismic accelerations, thus altering the inertial forces and the accumulated displacements, if any, depending on the strength and deformation characteristics of the medium. Several approaches such as the pseudo-static approach (Erzın and Cetin 2014, Sahoo and Shukla 2019), the pseudo-dynamic approach (Qin and Chian 2018, Nandi *et al*. 2021a, b), the displacement-based approach (Newmark 1965, Makdisi and Seed 1978, Ghanbari *et al*. 2013, Yuan *et al*. 2016), and the dynamic time-history approach (Prisco *et al*. 2011, Lu *et al*. 2014, Terzi and Selcuk 2015, Abe *et al*. 2017, Nasiri *et al*. 2020) are commonly used to address the effect of seismicity. Among all the methods mentioned above, the pseudo-static approach is widely recognized for its simplicity and efficiency in the seismic design of geotechnical structures (Eurocode 8, IS 1893), where uniform horizontal (k_hg) and vertical (k_vg) accelerations are considered throughout the soil domain. By representing a complex seismic phenomenon in the form of different uniform inertial forces throughout the soil domain, the pseudo-static approach aids engineers in solving various stability problems under seismic conditions.

*Corresponding author, Professor
E-mail: priyog@iitk.ac.in
[a]Research Scholar
[b]Assistant Professor

ISSN: 2005-307X (Print), 2092-6219 (Online)

The seismic analysis of retaining structures employing the pseudo-static approach was first demonstrated by Okabe (1926) and Mononobe and Matsuo (1929), and subsequently, it was popularized as the Mononobe-Okabe method. Different researchers (Terzaghi 1950, Majumdar 1971, Sarma 1973, Choudhury *et al*. 2007, Leshchinsky *et al*. 2012, Sahoo and Shukla 2019) implemented the Mononobe-Okabe method to address the seismic stability of slopes. Later, to relax the conservativeness involved in the pseudo-static approach, the pseudo-dynamic approach (Qin and Chian 2018, Nandi *et al*. 2021a, b) was developed by employing the site-specific dynamic soil properties such as shear modulus, damping ratio, and ground amplification. The deformation criterion governs the stability condition for slopes made of sufficiently soft materials. In such materials, the displacement-based approach (Newmark 1965, Makdisi and Seed 1978, Ghanbari *et al*. 2013, Yuan *et al*. 2016) is found to be more appealing for the evaluation of the permanently accumulated slope displacement. Among various seismic methods, the time-domain dynamic analysis (Prisco *et al*. 2011, Lu *et al*. 2014, Terzi and Selcuk 2015, Abe *et al*. 2017, Nasiri *et al*. 2020) captures the effect of large and complex earthquake events quite well. However, an exhaustive seismic analysis for a small project using such a rigorous approach is seldom performed in practice due to the higher cost and computational effort involved in the analysis. Moreover, the results obtained from the advanced techniques are sensitive to the choice of constitutive models and suitable dynamic boundary conditions, which demand more rigorous mathematical and computational efforts.

Since each seismic approach involves specific pros and cons based on some assumptions and idealizations, the feasibility of using these techniques in actual practice depends on various factors, such as the size of the project, the significance of the proposed structures, and the geological conditions of the site. By considering these facts, a simplistic approach for the seismic stability analysis of homogeneous slopes using the pseudo-static method is reported to be entirely legitimate by different researchers (Lee *et al*. 2017, Huang 2019). Besides, a comparative study by Yang *et al*. (2018) endorses a close agreement between the pseudo-static slope stability analysis using different design standards and the seismic time-history analysis. In addition, various design codes such as Eurocode 8, IS 1893, and experimental investigations (Lee *et al*. 2017, Huang 2019) also recommend the pseudo-static approach. Hence, the present investigation employs the classical pseudo-static approach to address the effect of earthquakes on slope stability analysis.

In most of the traditional slope stability analyses stated above, a possible slip surface such as a linear, circular, or logarithmic spiral was assumed prior to the analysis and then optimized to obtain the minimum factor of safety (Florkiewicz and Kubzdela 2013) or maximum permanent deformation (Ghanbari *et al*. 2013). However, the presumption of such slip surfaces might not reflect an accurate representation, especially under seismic conditions. While investigating the critical slip surface in the analysis, different search techniques based on optimization algorithms such as particle swarm optimization method (Su and Shao 2021), variational method (Sarkar and Chakraborty 2019), genetic algorithm (Li *et al*. 2009) were implemented in literature. However, the efficacy of the aforesaid methods relies on the accuracy of optimizing the objective function subject to the control variables. The stability and suitability of each algorithm and the ability to converge and escape from multiple local minima majorly depend on the initial trial slip surface and its nature, which may be defined as the constraints in the analysis. The computation time also depends on the choice of the optimization algorithm. Moreover, such optimization techniques search for possible solutions based on a given set of constraints but do not guarantee the best (Cheng *et al*. 2007). Simultaneously, to capture the actual slip surface and the deformation characteristics of slopes, a few investigations were conducted using more specific solution techniques such as FEM (Griffiths and Lane 1999, Li 2007, Khosravi *et al*. 2013). However, it is a fact that conventional FE analysis generally demands rigorous computational efforts to solve this class of problem without assuming any predefined slip surface. In contrast, the solution based on the slip line method, as proposed by Sokolovski (1960), can be an excellent choice to overcome the limitations associated with the rigorous optimization process and the computational efforts involved, even for the simple preliminary stability analysis. The inclusion of the slip line method in the analysis of various geotechnical stability problems (Sokolovski 1960, Kumar and Ghosh 2007, Veiskarami *et al*. 2011, Keshavarz and Kumar 2017, Li *et al*. 2019, Nandi *et al*. 2021a, b) also ensured an automatic generation of the failure surface. Nandi *et al*. (2021a, b) addressed the limiting stability of finite soil slopes under seismic conditions using the slip line theory along with the pseudo-dynamic methods. A reliable prediction for the seismic performance of finite soil slopes was made by deriving the slope geometries at the onset of the limiting equilibrium, that is, the factor of safety (FS) = 1.0. The concept of the extreme slope profile, thus proposed by Nandi *et al*. (2021a, b), superseded other conventional stability indices such as a factor of safety, critical earthquake acceleration, and limiting surcharge. The necessity of predefined slope geometries and failure surfaces was eliminated in the analysis. An efficient solution in the form of curvilinear slope faces was endowed in slope engineering. However, the mathematical rigor of the pseudo-dynamic methods involved in the analysis of Nandi *et al*. (2021a, b) often subdues the essence of the slip line theory. Hence, the efficacy of the slip line method combined with the simple but widely acclaimed pseudo-static approach (Okabe 1926, Mononobe and Matsuo 1929, Eurocode 8, IS 1893) demands immediate attention from researchers.

Consequently, the current investigation attempts to couple the slip line method with the pseudo-static approach for predicting the stability of slopes under seismic conditions. A numerical simulation of the extreme slope face was also performed using the finite element limit analysis (FELA) based software OptumG2 to reveal the authenticity of the proposed methodology. For a wide range

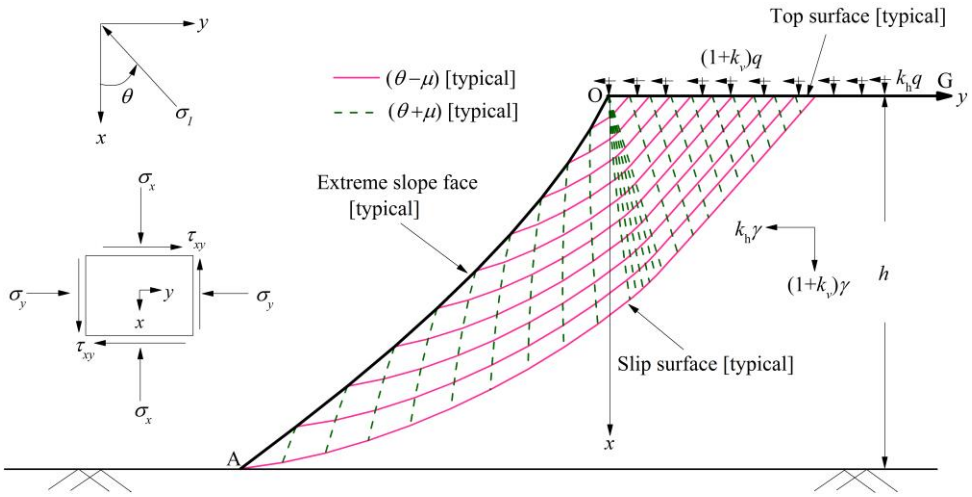

Fig. 1 Collapse mechanism and state of stress

of soil parameters and seismic accelerations, the current outcomes through the extreme slope face can serve as the design charts for geotechnical engineers to ensure the stability of slopes. By identifying the zone of instability in slopes, the present investigation can likewise show the requirement for remedial measures such as slope stabilization. Further, it can be conceived that such a non-linear slope face may be a substitute for traditional linear slopes from an economic perspective (Vahedifard *et al*. 2016). The application of the design charts is demonstrated by following the analysis to make the proposed approach effective for various geotechnical projects.

2. Definition of problem

This study considers a finite soil slope of height h to carry a uniform surcharge q on the horizontal top surface (Fig. 1). The soil with cohesion c, angle of internal friction ϕ, and unit weight γ is under the dry condition and assumed to follow the Mohr-Coulomb failure criterion. The main objective is to search for the slope geometry considering the limiting condition under the static and the seismic loadings, that is, FS = 1.0. The stability analysis was carried out using the slip line method in association with the pseudo-static approach.

3. Analysis

Among various theories developed from the stress plasticity approach, the mathematical formulations proposed by Hill (1950) marked the evolution of the slip line theory for metals and other potential plastic materials. Subsequently, Sokolovski (1960) developed a solution procedure to solve the stability-related problems in geotechnical engineering. Later, Graham (1968) provided an improved and detailed iterative procedure for the slip line method, which was popularly demonstrated as the method of stress characteristics and used by several researchers (Veiskarami *et al*. 2011, Keshavarz and Kumar 2017, Li *et al*. 2019) to solve various geotechnical problems.

3.1 Governing equations

A detailed description of this method and the solution procedure were already discussed by previous researchers (Graham 1968, Cheng and Au 2005, Peng and Chen 2013, Nandi *et al*. 2021a, b). However, a brief discussion on the slip line formulation is included here for the sake of its entirety. For a cohesive-frictional soil medium obeying the Mohr-Coulomb yield criterion, the state of stress at any point lying under the plastic equilibrium can be expressed as (Fig. 1),

$$\sigma_x = \sigma\left(1+\sin\phi\cos 2\theta\right) - c\cot\phi \tag{1a}$$

$$\sigma_y = \sigma\left(1-\sin\phi\cos 2\theta\right) - c\cot\phi \tag{1b}$$

$$\tau_{xy} = \sigma\sin\phi\sin 2\theta \tag{1c}$$

where σ is the distance between the centre of the Mohr circle and the point where the Coulomb failure envelope crosses the normal stress axis on the Mohr-stress diagram, and θ is the angle between the direction of the major principal stress and the positive x-axis with a counter-clockwise sense of rotation taken as positive, as shown in Fig. 1.

By imposing homogeneity and isotropy in the medium, the equilibrium equations under the plane strain condition can be written as

$$\frac{\partial\sigma_x}{\partial x} + \frac{\partial\tau_{xy}}{\partial y} = \gamma\left(1+k_v\right) \tag{2a}$$

$$\frac{\partial\tau_{xy}}{\partial x} + \frac{\partial\sigma_y}{\partial y} = -\gamma k_h \tag{2b}$$

where k_h and k_v are the non-dimensional earthquake acceleration coefficients obtained by normalizing the

horizontal ($k_h g$) and the vertical ($k_v g$) seismic accelerations with the acceleration due to gravity (g).

A pair of first-order quasi-linear differential equations can be derived by employing the Mohr-Coulomb yield criterion in Eq. (2). Following Sokolovski (1960), a solution for these quasi-linear equations can be obtained by generating the following set of ordinary differential equations, Eqs. (3(a)) and (3(b)) along ($\theta - \mu$) and ($\theta + \mu$) slip lines, respectively.

$$\frac{dy}{dx} = \tan(\theta - \mu); \frac{d\eta}{dx} = a \tag{3a}$$

$$\frac{dy}{dx} = \tan(\theta + \mu); \frac{d\xi}{dx} = b \tag{3b}$$

where

$$\left.\begin{matrix}\xi \\ \eta\end{matrix}\right\} = \left[\left(\left(\frac{\cot\phi}{2}\right)\ln\left(\frac{\sigma}{\sigma_0}\right)\right) \pm \theta\right]; \mu = \left(\frac{\pi}{4} - \frac{\phi}{2}\right)$$

$$\left.\begin{matrix}a \\ b\end{matrix}\right\} = \pm\frac{\gamma(1+k_v)\sin(\theta \pm \mu) + \gamma k_h \cos(\theta \pm \mu)}{2\sigma \sin\phi \cos(\theta \mp \mu)}$$

σ_0 is the characteristic stress, which can be any predefined value with the dimension of stress, and hence, it is chosen as the soil cohesion in this study.

3.2 Boundary conditions

Being a known boundary, the state of stress along the top surface (OG) is fully known (Fig. 1). Hence, the magnitude of θ and σ along OG (θ_t and σ_t) can be obtained as

$$\theta_t = -\frac{1}{2}\left(\psi + \sin^{-1}\left(\frac{\sin\psi}{\sin\phi}\right)\right) \tag{4a}$$

$$\sigma_t = \frac{q(1+k_v) + c\cot\phi}{1 + \sin\phi\cos 2\theta_t} \tag{4b}$$

where $\psi = \tan^{-1}\left[\frac{qk_h}{q(1+k_v) + c\cot\phi}\right] \le \phi$

Similarly, the magnitude of σ along the stress-free slope surface (OA) i.e., σ_s can be obtained as

$$\sigma_s = \frac{c\cot\phi}{(1-\sin\phi)} \tag{5a}$$

Since the major principal stress at any point on the slope surface should act along the tangent at that point, the magnitude of θ along OA (θ_s) can be expressed as

$$\frac{dy}{dx} = \tan\theta_s \tag{5b}$$

3.3 Extreme slope face

From Eqs. (4(b)) and (5(a)), it can be conceived that there exists a stress singularity at the slope crest (O) and hence, the magnitude of η becomes constant at O. By considering the constant nature of η at O, the magnitude of θ_s at O can be obtained as

$$\theta_s = \frac{\cot\phi}{2}\ln\left(\frac{\sigma_s}{\sigma_t}\right) + \theta_t \tag{6}$$

To avoid the stress discontinuity and maintain the numerical stability in the computation, the current analysis considers a minimum surcharge q applied on the top surface OG, which should satisfy the following inequality condition.

$$q \ge \frac{c\cos\phi(1+\cos 2\theta_t)}{(1-\sin\phi)(1+k_v)} \tag{7}$$

The state of stress on the top surface is fully known by satisfying the available boundary conditions. Besides, it can be understood from Eqs. (5(a))-(5(b)) that the magnitude of θ_s varies along the stress-free slope face. Hence, the slip lines emerging from the top surface (OG) proceed towards the slope face (OA) using a finite difference scheme as described by Sokolovski (1960) and Kumar and Ghosh (2007), which eventually establish the extreme geometry of slopes with FS = 1.0 under both static and seismic conditions.

4. Results

Unlike other traditional methods, the present analysis looks for the extreme slope face for given soil properties, surcharge loading, and seismic accelerations. Computer code was developed in MATLAB to perform the present numerical analysis for a range of parameters such as ϕ = 25° to 45°, $c/\gamma h$ = 0.075 to 0.15, k_h = 0 to 0.3, and k_v = ($-0.5k_h$) to k_h.

4.1 Stability charts

The extreme slope faces developed for a range of input parameters such as k_h, ϕ, $c/\gamma h$, and $q/\gamma h$ are presented in Figs. 2 and 3. It can be observed that the extreme profile of slopes tends to be flattened with an increase in horizontal seismic acceleration. However, from Figs. 2 and 3, it can be realized that slopes can adopt steeper configurations through the enhancement of the shear strength parameters of soil (c and ϕ). Hence, the charts depicted in Figs. 2 and 3 can be utilized to assess the stability of existing or proposed slopes. In addition to the stability analysis, these charts may provide important information about more economical slope geometry, such as curvilinear or bi-linear slope faces.

4.2 Effect of direction of seismic accelerations

It is worth noting that during a seismic investigation, the direction of the horizontal and the vertical accelerations mainly depends on the critical condition. From the law of mechanics, it tends to be perceived that slopes are more vulnerable when the horizontal seismic acceleration acts towards the slope face, with the vertical seismic acceleration acting downward. Conversely, Kolathayar and Ghosh (2009) reported that the upward direction of the vertical seismic acceleration sometimes became critical.

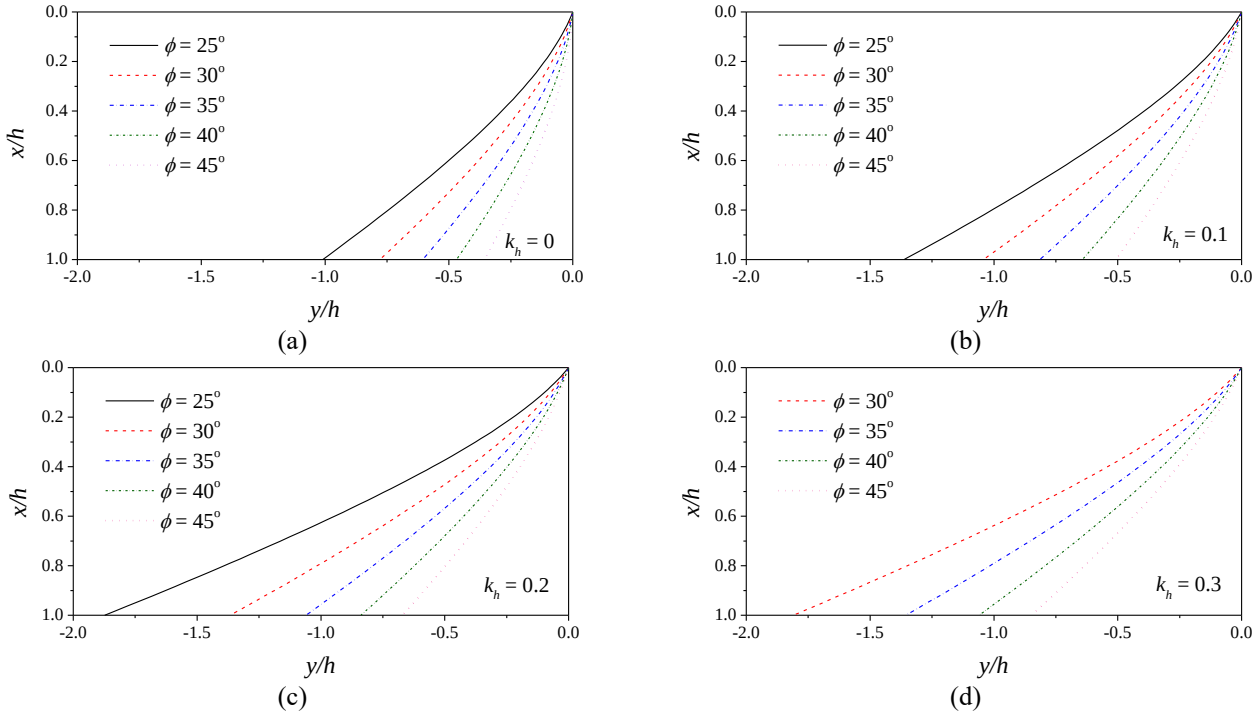

Fig. 2 Extreme slope faces for different values of ϕ with $c/\gamma h = 0.075$, $q/\gamma h = 0.4$, $k_v = 0.5k_h$: (a) $k_h = 0$, (b) $k_h = 0.1$, (c) $k_h = 0.2$; and (d) $k_h = 0.3$

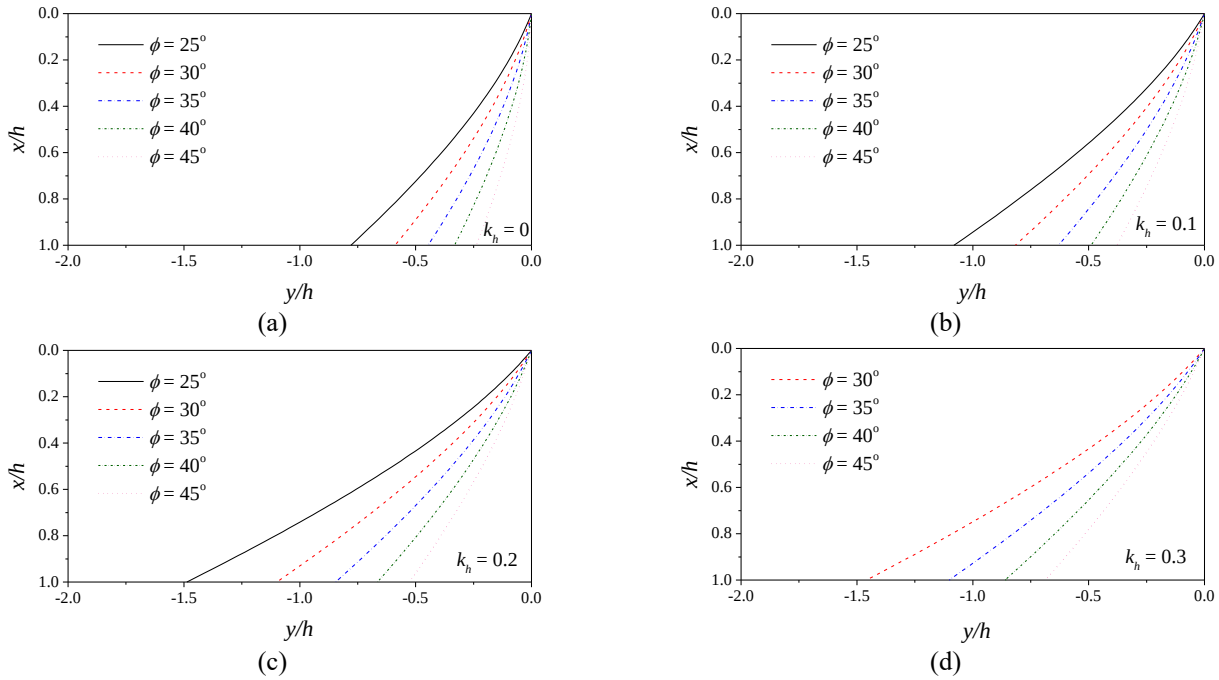

Fig. 3 Extreme slope faces for different values of ϕ with $c/\gamma h = 0.15$, $q/\gamma h = 0.8$, $k_v = 0.5k_h$: (a) $k_h = 0$, (b) $k_h = 0.1$, (c) $k_h = 0.2$; and (d) $k_h = 0.3$

Hence, in the present investigation, a parametric study was conducted to search for the critical direction of the vertical seismic acceleration. The effect of k_h and k_v on the extreme geometry of slopes is presented in Figs. 4 and 5, respectively. It can be observed from Fig. 4 that the horizontal seismic acceleration (k_h) severely affects the geometry of slopes. In Fig. 5, the extreme slope geometry is found to be flat throughout the slope face as k_v is assumed to act downward with k_h varying from 0 to 0.2. However, at $k_h = 0.3$ and beyond $x/h = 0.7$, the critical direction of the vertical seismic acceleration shifts from downward to upward. Hence, it can be conceived that the critical direction of k_v may assume the upward direction at a higher seismicity level ($k_h > 0.3$) as reported by previous researchers (Greco 2008, Kolathayar and Ghosh 2009). From Fig. 5, it can also be noted that the effect of the

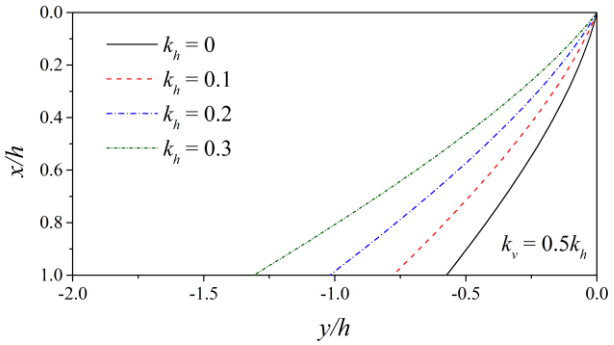

Fig. 4 Variation of extreme slope face at different values of k_h with $\phi = 35°$, $c/\gamma h = 0.1$, $q/\gamma h = 0.6$

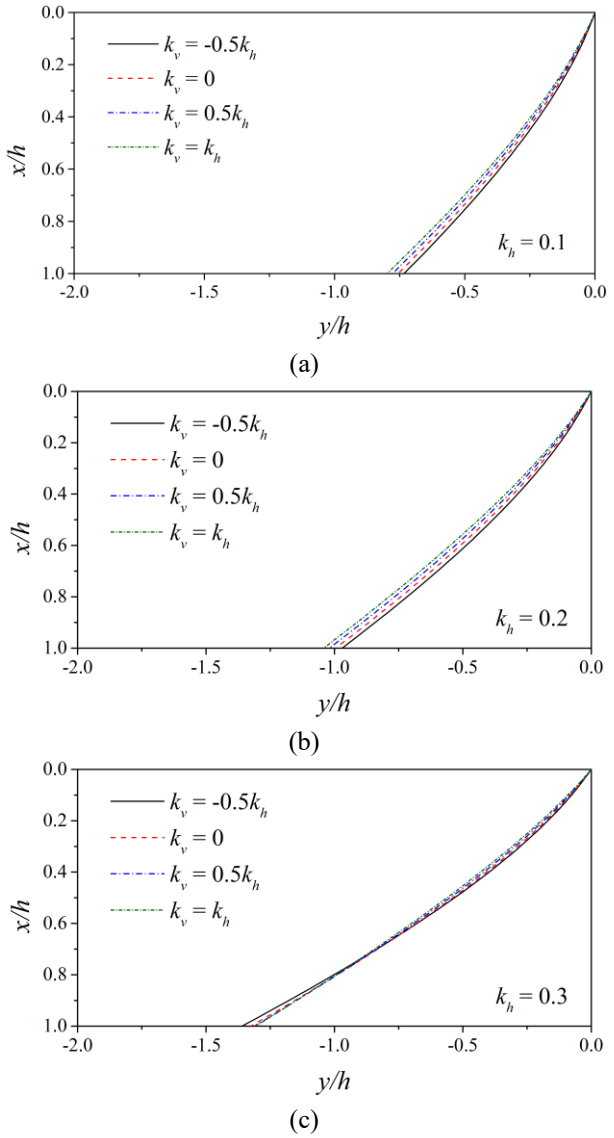

Fig. 5 Variation of extreme slope face at different values k_v with $\phi = 35°$, $c/\gamma h = 0.1$, $q/\gamma h = 0.6$ (a) $k_h = 0.1$, (b) $k_h = 0.2$; and (c) $k_h = 0.3$

direction of k_v on the slope configuration turns out to be nominal. This might be a reason to neglect the effect of k_v in earlier studies (Majumdar 1971, Sarma 1973, Erzın and Cetin 2014). Nevertheless, the present design charts (Figs. 2 and 3) are generated considering k_v in the downward direction with a magnitude of $0.5k_h$.

4.3 Slip surfaces and stress contours

With the known state of stress developed within the plastic domain, the slip surface and the stress contour for slopes can be traced in the current analysis. From Fig. 6, it can be observed that the size of the plastic domain increases with an increase in the magnitude of k_h, which may be attributed to the greater seismic inertial forces. It is imperative to specify that the slip surface (AG) obtained from the analysis is neither linear nor circular. Instead, the shape of the curve is automatically evolved from the slip line solution. In addition, the stress mobilization in the plastic domain under static and seismic conditions is presented through the normalized stress contours in Fig. 6. It can be noticed from Fig. 6 that the stability of the extreme slope face is established through a gradual decrease in the magnitude of $\sigma/\gamma h$ from the slip surface to the stress-free slope face.

5. Comparison

The majority of the available theories emphasized the seismic stability of slopes with a given geometry in terms of either *FS*, limiting surcharge, or yield acceleration. However, the present methodology advocates for the extreme slope face as the stability index for a given set of soil properties. Hence, a direct comparison is difficult to obtain. Nonetheless, a qualitative comparison was conducted by searching for extreme slope faces for the limiting surcharge and the limit-state shear strength parameters of the soil, as recommended by Qin and Chian (2018) and Cui *et al*. (2022), respectively. It is worth mentioning that Qin and Chian (2018) performed the investigation using the upper-bound limit analysis, whereas Cui *et al*. (2022) utilized the limit equilibrium analysis. For the input parameters adopted by Qin and Chian (2018) and Cui *et al*. (2022), the extreme slope geometries are produced using the present concept, as shown in Figs. 7 and 8. In Figs. 7 and 8, the linear slope profiles of Qin and Chian (2018) and Cui *et al*. (2022) with a horizontal inclination (α) of 50° and 45°, respectively are generally found to be conservative (flat slope) compared to the present extreme curvilinear slope configurations.

A case study on the seismic stability of the III zone of the Longnan slope (Qian and Zou 2022) is considered to validate the current methodology. The Longnan slope is located in the Huining-Wudu seismic belt adjacent to the Songpan-Pingwu seismic belt in China. By determining the critical *FS*, Qian and Zou (2022) forecasted a potential Longnan slope collapse under the Wenchuan earthquakes (2008) using the three-dimensional upper-bound limit analysis alongside the modified pseudo-dynamic approach. In Fig. 9, an attempt is made to derive the extreme geometries of the Longnan slope under static and seismic conditions using the inputs adopted by Qian and Zou (2022). Qian and Zou (2022) classified the Wenchuan

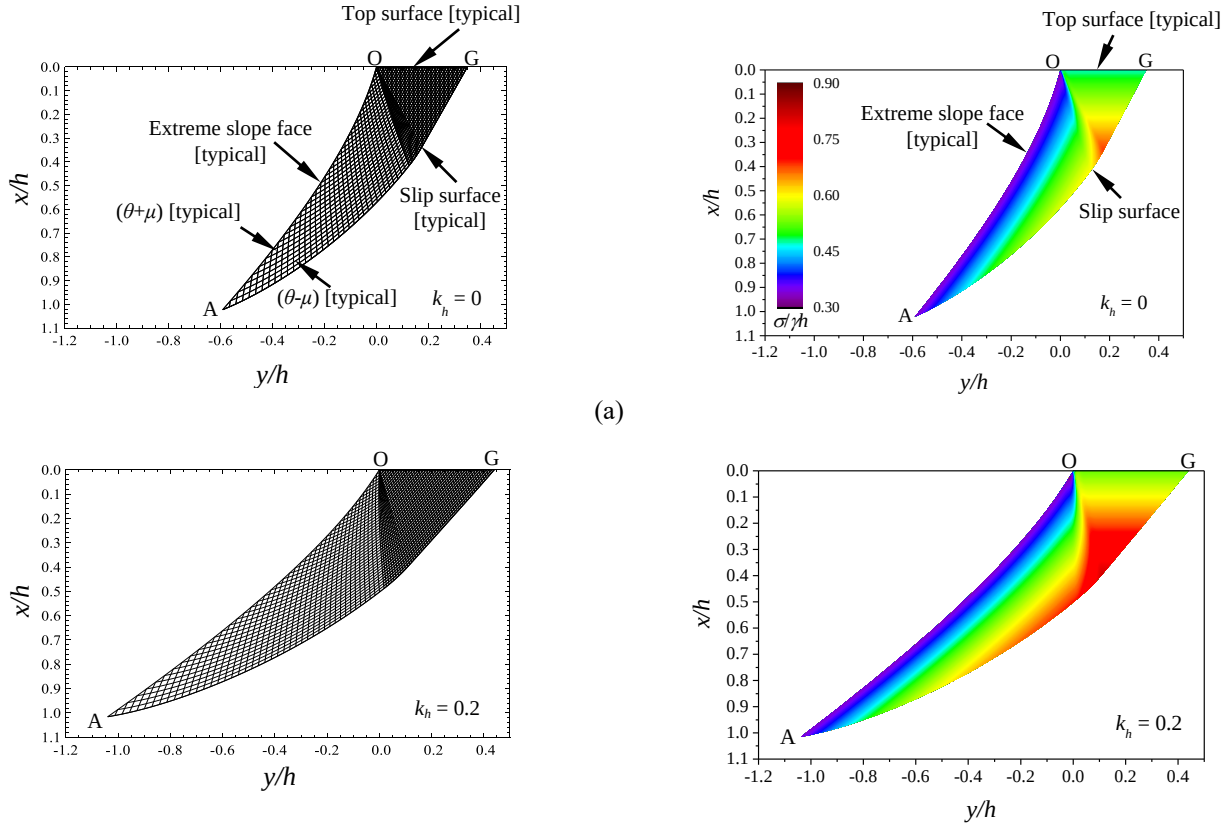

Fig. 6 Slip surfaces and stress contours for slope with $\phi = 35°$, $c/\gamma h = 0.1$, $q/\gamma h = 0.6$, $k_v = 0.5k_h$: (a) static condition; and (b) seismic condition

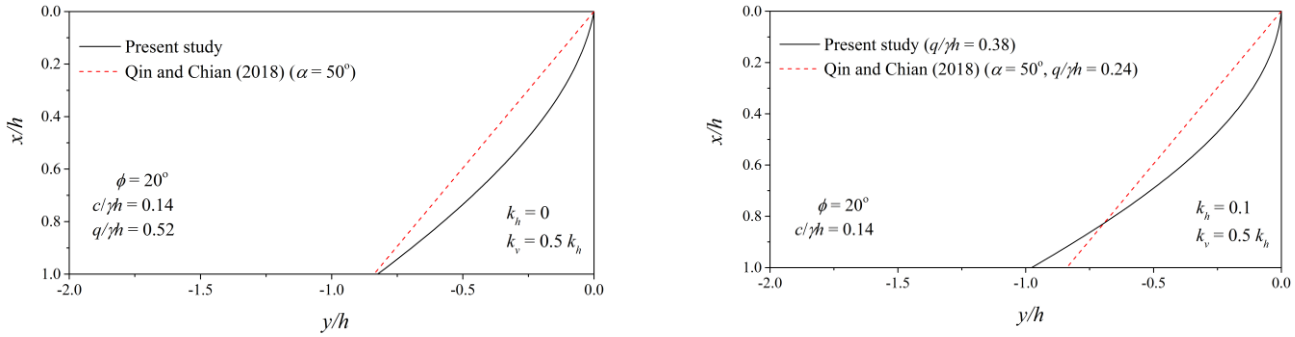

Fig. 7 Comparison of present slope surfaces with the linear slopes of Qin and Chian (2018) for $\phi = 20°$, $c/\gamma h = 0.14$, $k_v = 0.5k_h$: (a) static condition; and (b) seismic condition

earthquakes into low-level, medium-level, and high-level earthquakes by considering the seismic intensity. The pseudo-static acceleration coefficients corresponding to the aforesaid seismic levels, as mentioned in Fig. 9, can be found in Zhou and Cheng (2014). From a qualitative comparison shown in Fig. 9(a), the Longnan slope ($\alpha = 55°$) matches closely with the derived extreme slope face (*FS* = 1.0) and is found to be marginally stable. This is in line with the critical *FS* value of 1.0351 as determined by Qian and Zou (2022) under static conditions. However, as the seismic intensity level increases (Figs. 9(b)-9(d)), the extreme slope faces acquire a flat configuration compared to the Longnan slope ($\alpha = 55°$) due to increased seismic inertial forces induced in the medium. Consequently, the Longnan slope no longer satisfies the condition of the limiting stability (*FS* = 1.0). Instead, it becomes susceptible to failure, as Qian and Zou (2022) predicted for low-level, medium-level, and high-level earthquakes with the critical *FS* of 0.6541, 0.2754, and 0.1933, respectively. Thus, despite the simplicity of the present method, a qualitative but reliable assessment of the seismic slope stability can be achieved without an exhaustive computational effort.

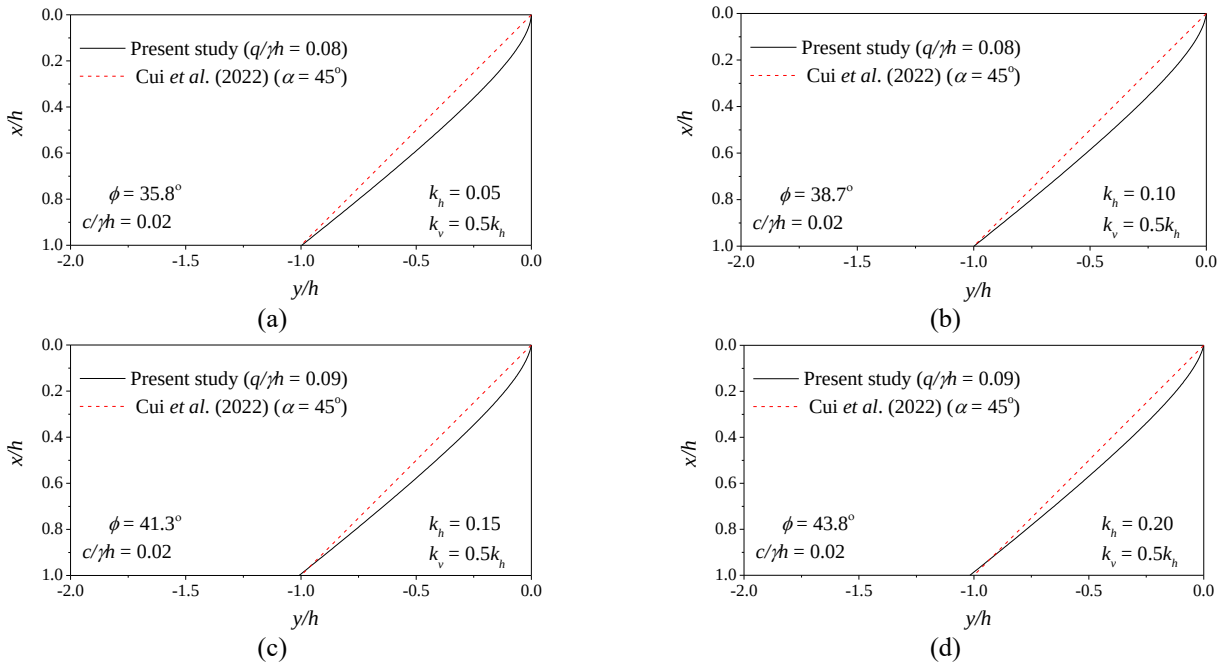

Fig. 8 Comparison of present slope surfaces with the linear slopes of Cui *et al.* (2022): (a) k_h = 0.05, (b) k_h = 0.10, (c) k_h = 0.15; and (d) k_h = 0.20

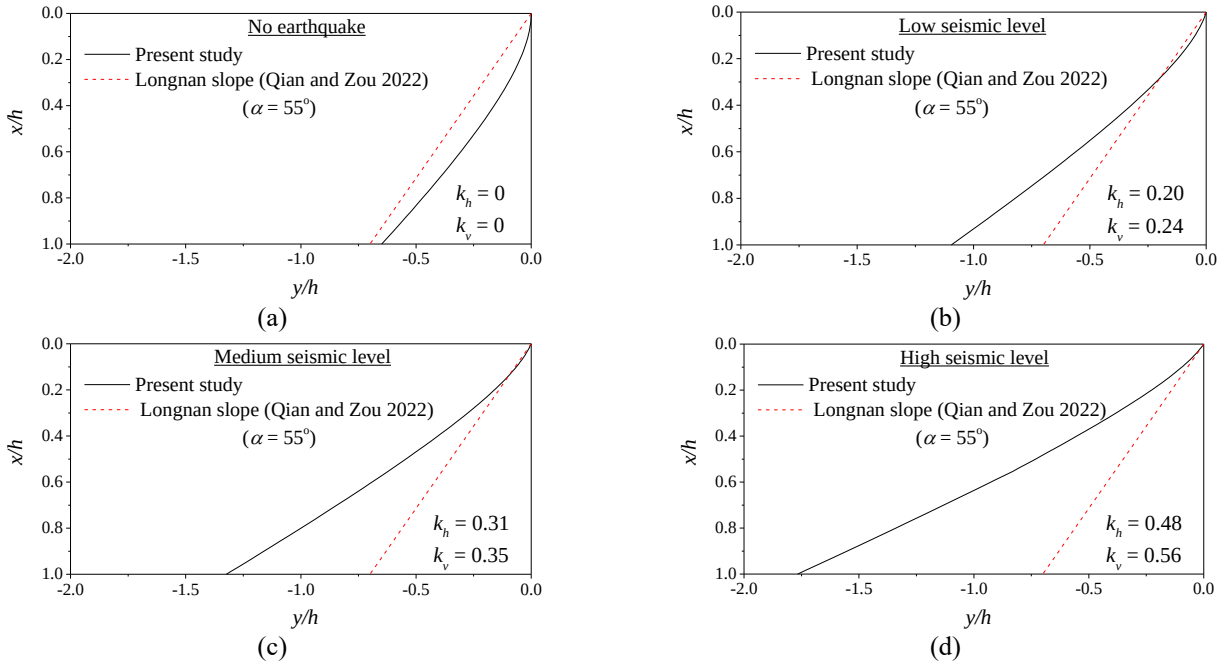

Fig. 9 Comparison of present slope surfaces with the Longnan slope (Qian and Zou 2022) for ϕ = 38°, $c/\gamma h$ = 0.04, $q/\gamma h$ = 0.15: (a) no earthquake condition (k_h = 0, k_v = 0), (b) low seismic level condition (k_h = 0.20, k_v = 0.24), (c) medium seismic level condition (k_h = 0.31, k_v = 0.35); and (d) high seismic level condition (k_h = 0.48, k_v = 0.56)

Further, the proposed slip line-based methodology is compared with the results obtained from OptumG2, a commercially available finite element limit analysis (FELA) software (Krabbenhoft *et al*. 2015). The input parameters adopted for the comparison are summarized in Table 1. For the input parameters given in Table 1, the extreme slope face obtained from the present slip line approach was modeled with OptumG2. The inbuilt adaptive mesh refinement option available in OptumG2 was utilized to characterize the effect of a mesh configuration, as shown in Fig. 10(a). A representative shear dissipation pattern for the derived slope under seismic conditions (k_h = 0.1) is shown in Fig. 10(b). Further, the magnitudes of *FS* for the slope profiles derived from the slip line method under different seismic conditions are determined using OptumG2, and the results are tabulated in Table 2. It can be seen from Table 2 that the FELA solutions obtained from OptumG2 converge with the limiting *FS* ensured by the present slip line

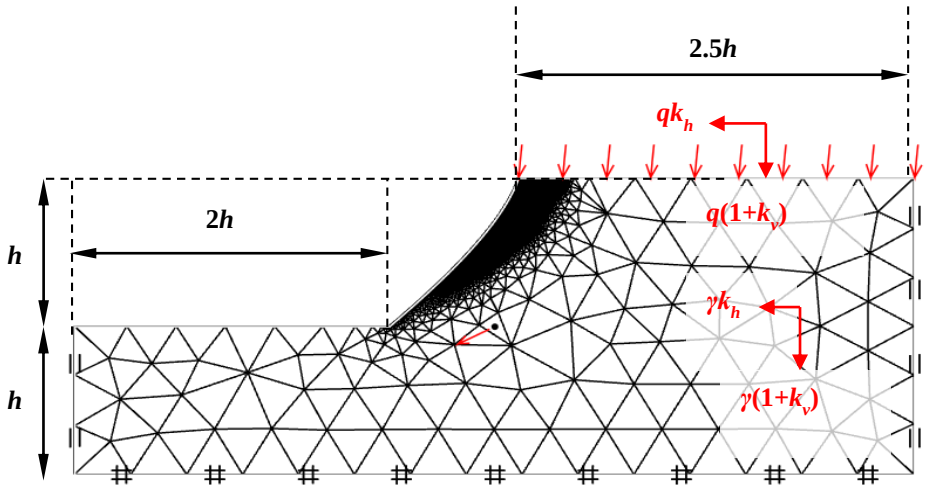

(a)

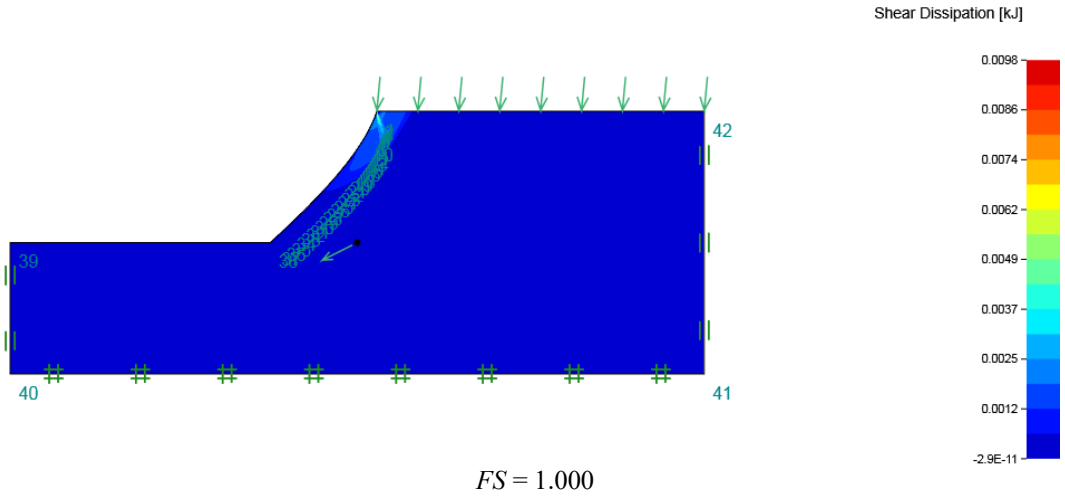

$FS = 1.000$

(b)

Fig. 10 (a) Typical FELA mesh using OptumG2 and (b) shear dissipation for the derived slope profile at $k_h = 0.1$

approach.

Since a direct comparison seems difficult from two different slope configurations, the extent of variation is measured in terms of root mean square deviation (*RMSD*) for N number of data points along the slope face, using Eq. (8).

$$RMSD = \sqrt{\frac{\sum_{i=1}^{N}(y_{ci} - y_{li})^2}{N}} \tag{8}$$

where (x_i , y_{ci}) and (x_i , y_{li}) are the Cartesian coordinates of the i^{th} data point along the extreme slope face and the known linear slope configuration, respectively, as shown in Fig. 11.

In this comparison, an *RMSD* of 0.06 to 0.10 can be observed between the derived slope geometries and the linear slope configurations (α = 50° and 45°) analyzed by Qin and Chian (2018) and Cui *et al*. (2022). This may be attributed to the fact that the results based on the slip line method are generally seen to fall between the lower and the upper bound solutions, and the partial fulfilment of the

Table 1 Input parameters considered in the analysis

Parameters	
Modulus of elasticity E (MPa)	30
Poisson ratio υ	0.25
Friction angle ϕ (°)	35
Cohesion c (kPa)	13.5
Unit weight γ (kN/m^3)	18
Slope height h (m)	10
Horizontal seismic coefficient k_h	0 – 0.3
Vertical seismic coefficient k_v	0.5k_h
Uniform surcharge q (kPa)	72
Material model	Mohr-Coulomb yield criterion with associative flow rule

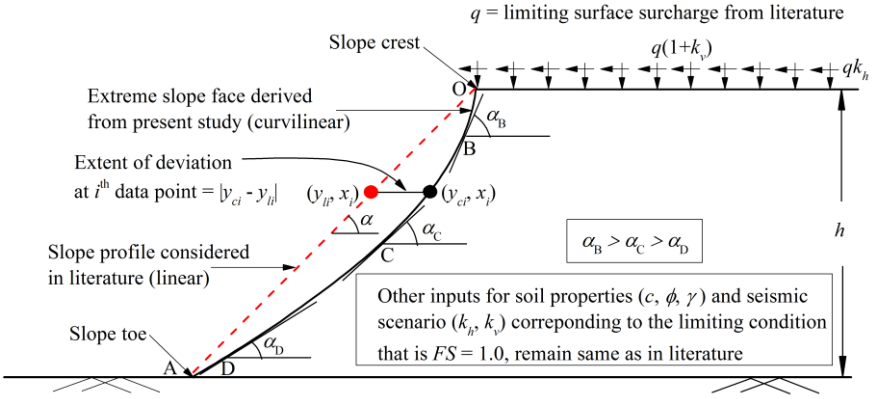

Fig. 11 Comparison of extreme slope face with linear slope using *RMSD*

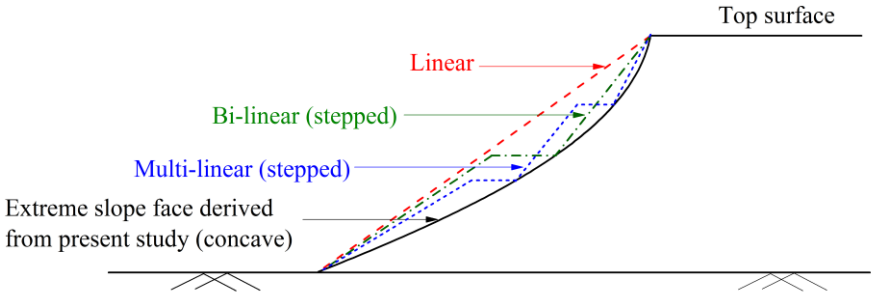

Fig. 12 Possible applications of derived slope geometry in practice

Table 2 Comparison of present slip line method with finite element limit analysis

k_h	k_v	*FS*	
		Slip line method	Finite element limit analysis
0.0	$0.5k_h$	1.000	1.001
0.1		1.000	1.000
0.2		1.000	1.001
0.3		1.000	1.000

limiting surcharge condition specified in Eq. (7) gets ensured. Additionally, Cui *et al*. (2022) presumed the failure surface to be circular while deriving the stability charts in the presence of seismic impact. Though there exists a marginal difference in the magnitude of $q/\gamma h$ considered in the comparison, it can be qualitatively noted from Fig. 7(b) that a portion of the linear slope considered by Qin and Chian (2018) turns out to be unsafe beyond x/h = 0.83, that is, flat compared to the extreme slope face prescribed by the slip line method.

6. Applications

The evaluated extreme slope face can be seen as curvilinear. However, the implementation of such curvilinear slope profiles seems problematic in practice. Hence, this section discusses the possible application of the present analysis to assess the stability of new and existing slopes.

- *Design guidelines for new slopes to be constructed*

The extreme slope face computed in this study serves as a demarcation between the zone of stability and instability. Obviously, for the given soil properties and seismic conditions, the proposed slope profile on the flat side (left side) of the derived extreme slope face ensures a stable configuration and vice-versa. Hence, by keeping this in mind, geotechnical engineers can proceed with any other slope configuration such as bi-linear or multi-linear (Fig. 12), which can provide an economically viable solution without compromising stability. Based on the input parameters given in Table 1, the present curvilinear slope profile can be modeled as equivalent linear or bi-linear geometry, as shown in Fig. 13. It is worth mentioning that the equivalent linear and bi-linear slope profiles shown in Fig. 13(a) were modeled in OptumG2, and the corresponding *FS* values were 1.002 and 1.011, respectively. Similarly, the slope geometry can further be optimized with a multi-linear slope. Hence, practicing engineers can effectively use the concept of a multi-linear slope profile along with the proposed design charts (Figs. 2 and 3) to optimize the slope profile.

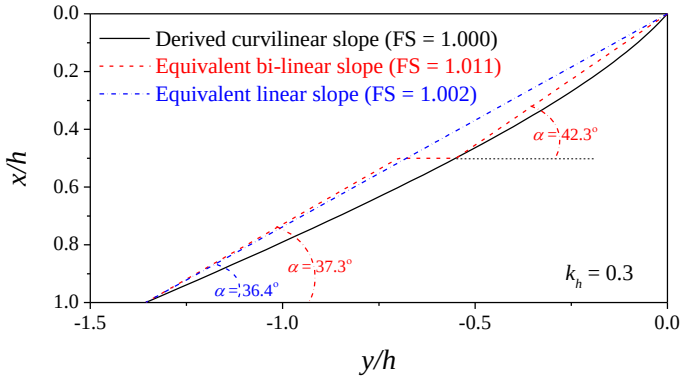

(a)

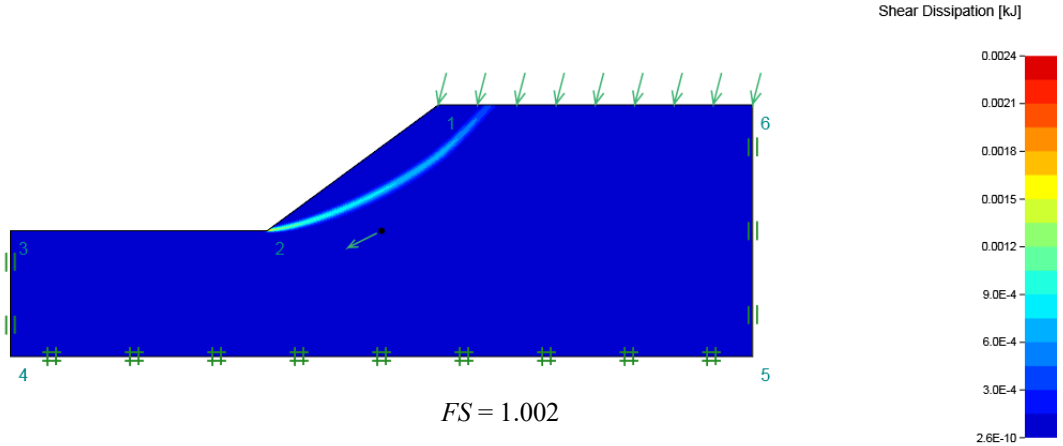

(b)

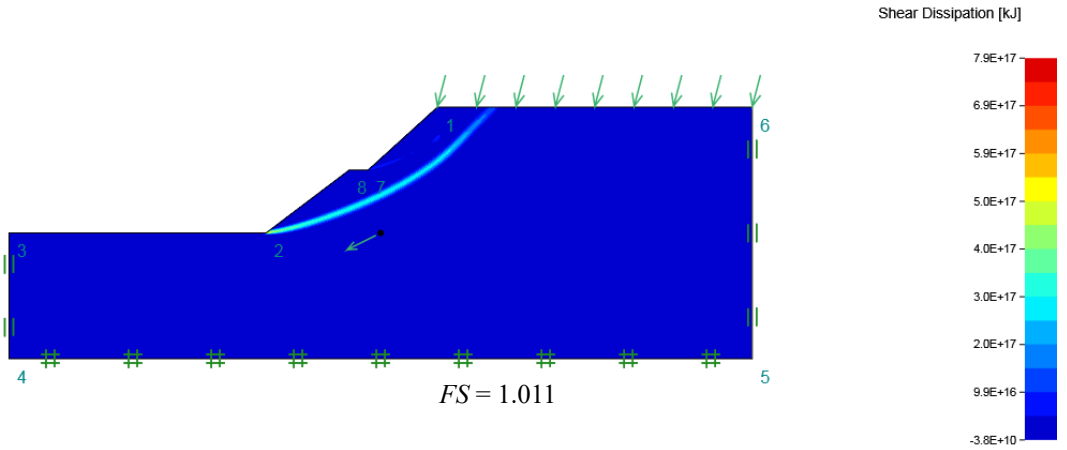

(c)

Fig. 13 FE limit analysis of linear and bi-linear slopes: (a) derivation of equivalent linear and bi-linear slopes from curvilinear slope, (b) shear dissipation for equivalent linear slope; and (c) shear dissipation for equivalent bi-linear slope

- *Indicator to take preventive measures for existing slopes*

Since the derived extreme slope profile acts as the benchmark to identify the weaker zone in a slope, indicating the need for stabilization over the specific portions of the slope. By comparing the existing slope configuration with the derived extreme slope face, the zone of instability can be identified, as demonstrated in Fig. 14. By adopting suitable slope strengthening techniques such as placing the reinforcement in the zone of instability, the stability of slopes can be regained.

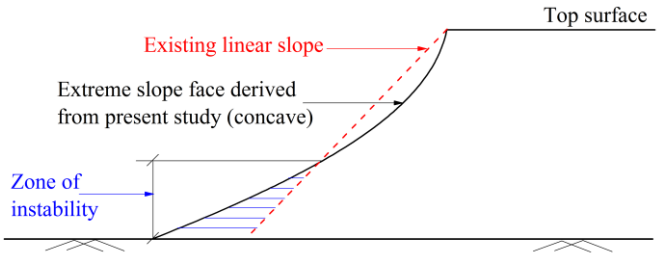

Fig. 14 Assessment of slope stability in existing slopes

7. Conclusions

The extreme slope face is obtained under seismic conditions by employing the slip line method in association with the pseudo-static approach. No predefined slip surface is assumed in the analysis. Despite a rigorous mathematical formulation, the present methodology does not demand any optimization study to determine the minimum *FS* as adopted in other classical approaches, such as the limit equilibrium and the limit analysis methods. The current approach provides a reliable and convincing estimate for assessing the seismic slope stability through validation with the rigorous finite element limit analysis. Along with a brief parametric study, the extreme slope face design charts are provided for a range of c-ϕ soils under different loading conditions. Such design charts can be helpful to practicing engineers in assessing the stability of existing slopes qualitatively and taking necessary remedial measures. This study advocates for the slope design with multi-linear slope geometry to achieve a more economical and stable profile.

Acknowledgments

The first author acknowledges the Ministry of Education, Government of India, for Prime Minister's Research Fellowship grant.

References

Abe, K., Nakamura, S., Nakamura, H. and Shiomi, K. (2017), "Numerical study on dynamic behavior of slope models including weak layers from deformation to failure using material point method", *Soils Found.*, **57**(2), 155-175. https://doi.org/10.1016/j.sandf.2017.03.001.

Bishop, A.W. (1955), "The use of the slip circle in the stability analysis of slopes", *Géotechnique*, **5**(1), 7-17. https://doi.org/10.1680/geot.1955.5.1.7.

Cheng, Y.M. and Au, S.K. (2005), "Solution of the bearing capacity problem by the slip line method", *Can. Geotech. J.*, **42**(4), 1232-1241. https://doi.org/10.1139/t05-037.

Cheng, Y.M., Li, L. and Chi, S.C. (2007), "Performance studies on six heuristic global optimization methods in the location of critical slip surface", *Comput. Geotech.*, **34**(6), 462-484. https://doi.org/10.1016/j.compgeo.2007.01.004.

Choudhury, D., Basu, S. and Bray, J.D. (2007), "Behaviour of slopes under static and seismic conditions by limit equilibrium method", *Proceedings of Geo-Denver 2007: New Peaks in Geotechnics*, Denver, Colorado, February.

Cui, H., Ji, J., Song, J. and Huang, W. (2022), "Limit state line-based seismic stability charts for homogeneous earth slopes", *Comput. Geotech.*, **146**, 104749. https://doi.org/10.1016/j.compgeo.2022.104749.

Erzın, Y. and Cetin, T. (2014), "The prediction of the critical factor of safety of homogeneous finite slopes subjected to earthquake forces using neural networks and multiple regressions", *Geomech. Eng.*, **6**(1), 1-15. https://doi.org/10.12989/gae.2014.6.1.001.

Eurocode 8 (2004), Design of structures for earthquake resistance. Part 5: Foundations, retaining structures and geotechnical aspects, European Committee for Standardization; Brussels, Belgium.

Fellenius, W. (1936), "Calculation of the stability of earth dams", *Proceedings of Transactions of the 2nd Congress on Large Dams, International Commission on Large Dams of the World Power Conference*, Washington, DC, December.

Florkiewicz, A. and Kubzdela, A. (2013), "Factor of safety in limit analysis of slopes", *Geomech. Eng.*, **5**(5), 485-497. https://doi.org/10.12989/gae.2013.5.5.485.

Ghanbari, A., Khalilpasha, A., Sabermahani, M. and Heydari, B. (2013), "An analytical technique for estimation of seismic displacements in reinforced slopes based on horizontal slices method (HSM)", *Geomech. Eng.*, **5**(2), 143-164. https://doi.org/10.12989/gae.2013.5.2.143.

Graham, J. (1968), "Plane plastic failure in cohesionless soils", *Géotechnique*, **18**(3), 301-316. https://doi.org/10.1680/geot.1968.18.3.301.

Gray, D.H. (2013), "Influence of slope morphology on the stability of earthen slopes", *Proceedings of the Geo-Congress 2013: Stability and Performance of Slopes and Embankments*, San Diego, California, March.

Greco, V.R. (2008), "Discussion of seismic active earth pressure behind a nonvertical retaining wall using pseudo-dynamic analysis", *Can. Geotech. J.*, **45**(12), 1795-1797. https://doi.org/10.1139/T08-099.

Griffiths, D.V. and Lane, P.A. (1999), "Slope stability analysis by finite elements", *Géotechnique*, **49**(3), 387-403. https://doi.org/10.1680/geot.1999.49.3.387.

Hill, R. (1950), *The Mathematical Theory of Plasticity*, Oxford University Press, Oxford, UK.

Huang, C.C. (2019), "Experimental verification of seismic bearing capacity of near-slope footings using shaking table tests", *J. Earthq. Eng.*, https://doi.org/10.1080/13632469.2019.1665148.

IS 1893 (2016), Criteria for earthquake resistant design of structures. Part 1: General provisions and buildings, Bureau of Indian Standards; New Delhi, India.

Jeldes, I.A., Drumm, E.C. and Yoder, D.C. (2015), "Design of stable concave slopes for reduced sediment delivery", *J.*

Geotech. Geoenviron. Eng., **141**(2), 04014093-1-10. https://doi.org/10.1061/(ASCE)GT.1943-5606.0001211.

Keshavarz, A. and Kumar, J. (2017), "Bearing capacity computation for a ring foundation using the stress characteristics method", *Comput. Geotech.*, **89**, 33-42. https://doi.org/10.1016/j.compgeo.2017.04.006.

Khosravi, M., Leshchinsky, D., Meehan, C.L. and Khosravi, A. (2013), "Stability analysis of seismically loaded slopes using finite element techniques", *Proceedings of the Geo-Congress 2013: Stability and Performance of Slopes and Embankments*, San Diego, California, March.

Kolathayar, S. and Ghosh, P. (2009), "Seismic active earth pressure on walls with bilinear backface using pseudo-dynamic approach", *Comput. Geotech.*, **36**(7), 1229-1236. https://doi.org/10.1016/j.compgeo.2009.05.015.

Krabbenhoft, K., Lyamin, A. and Krabbenhoft, J. (2015), Optum Computational Engineering (OptumG2). https://optumce.com

Kumar, J. and Ghosh, P. (2007), "Ultimate bearing capacity of two interfering rough strip footings", *Int. J. Geomech.*, **7**(1), 53-62. https://doi.org/10.1061/(ASCE)1532-3641(2007)7:1(53).

Lee, M.G., Ha, J.G., Jo, S.B., Park, H.J. and Kim, D.S. (2017), "Assessment of horizontal seismic coefficient for gravity quay walls by centrifuge tests", *Géotechnique Lett.*, **7**(2), 211-217. https://doi.org/10.1680/jgele.17.00005.

Leshchinsky, D., Ebrahimi, S., Vahedifard, F. and Zhu, F. (2012), "Extension of Mononobe–Okabe approach to unstable slopes", *Soils Found.*, **52**(2), 239-256. https://doi.org/10.1016/j.sandf.2012.02.004.

Li, C., Jiang, P. and Zhou, A. (2019), "Rigorous solution of slope stability under seismic action", *Comput. Geotech.*, **109**, 99-107. https://doi.org/10.1016/j.compgeo.2019.01.018.

Li, S., Shangguan, Z., Duan, H., Liu, Y. and Luan, M. (2009), "Searching for critical failure surface in slope stability analysis by using hybrid genetic algorithm", *Geomech. Eng*., **1**(1), 85-96. https://doi.org/10.12989/gae.2009.1.1.085.

Li, X. (2007), "Finite element analysis of slope stability using a nonlinear failure criterion", *Comput. Geotech.*, **34**(3), 127-136. https://doi.org/10.1016/j.compgeo.2006.11.005.

Lu, L., Wang, Z., Huang, X., Zheng, B. and Arai, K. (2014), "Dynamic and static combination analysis method of slope stability analysis during earthquake", *Math. Probl. Eng*., Article ID 573962. https://doi.org/10.1155/2014/573962.

Majumdar, D.K. (1971), "Stability of soil slopes under horizontal earthquake force", *Géotechnique*, **21**(1), 84-88. https://doi.org/10.1680/geot.1971.21.1.84.

Makdisi, F.I. and Seed, H.B. (1978), "Simplified procedure for estimating dam and embankment earthquake-induced deformations", *J. Geotech. Eng. Div.*, **104**(7), 849-867. https://doi.org/10.1061/AJGEB6.0000668.

Mononobe, N. and Matsuo, H. (1929), "On the determination of earth pressures during earthquakes", *Proceedings of the World Engineering Conference*, Tokyo.

Nandi, S., Santhoshkumar, G. and Ghosh, P. (2021a), "Determination of critical slope face in *c–ϕ* soil under seismic condition using method of stress characteristics", *Int. J. Geomech.*, **21**(4), 04021031-1-13. https:// https://doi.org/10.1061/(ASCE)GM.1943-5622.0001976.

Nandi, S., Santhoshkumar, G. and Ghosh, P. (2021b), "Development of limiting soil slope profile under seismic condition using slip line theory", *Acta Geotechnica*, **16**(11), 3517-3531. https://doi.org/10.1007/s11440-021-01251-4.

Nasiri, F., Javdanian, H. and Heidari, A. (2020), "Seismic response analysis of embankment dams under decomposed earthquakes", *Geomech. Eng*., **21**(1), 35-51. https://doi.org/10.12989/gae.2020.21.1.035.

Newmark, N.M. (1965), "Effects of earthquakes on dams and embankments", *Géotechnique*, **15**(2), 139-160. https://doi.org/10.1680/geot.1965.15.2.139.

Okabe, S. (1926), "General theory of earth pressures", *J. Japan Soc. Civ. Eng*., **12**, 1277-1323.

Peng, M.X. and Chen, J. (2013), "Slip-line solution to active earth pressure on retaining walls", *Géotechnique*, **63**(12), 1008-1019. https://doi.org/10.1680/geot.11.P.135.

Prisco, C.di., Pastor, M. and Pisanò, F. (2012), "Shear wave propagation along infinite slopes: a theoretically based numerical study", *Int. J. Numer. Anal. Meth. Geomech.*, **36**(5), 619-642. https://doi.org/10.1002/nag.1020.

Qian. Z.H. and Zou, J.F. (2022), "Three-dimensional rigorous upper-bound limit analysis of soil slopes subjected to variable seismic excitations", *Comput. Geotech*., **147**, 104714. https://doi.org/10.1016/j.compgeo.2022.104714.

Qin, C.-B. and Chian, S.C. (2018), "Kinematic analysis of seismic slope stability with a discretisation technique and pseudo-dynamic approach: a new perspective", *Géotechnique*, **68**(6), 492-503. https://doi.org/10.1680/jgeot.16.P.200.

Rieke-Zapp, D.H. and Nearing, M.A. (2005), "Slope shape effects on erosion: a laboratory study", *Soil Sci. Soc. Am. J.*, **69**(5), 1463-1471. https://doi.org/10.2136/sssaj2005.0015.

Sahoo, P.P. and Shukla, S.K. (2019), "Taylor's slope stability chart for combined effects of horizontal and vertical seismic coefficients", *Géotechnique*, **69**(4), 344-354. https://doi.org/10.1680/jgeot.17.P.222.

Sarkar, S. and Chakraborty, M. (2019), "Pseudostatic slope stability analysis in two-layered soil by using variational method", *Proceedings of the 7th International Conference on Earthquake Geotechnical Engineering*, Rome, Italy, June.

Sarma, S.K. (1973), "Stability analysis of embankments and slopes", *Géotechnique*, **23**(3), 423-433. https://doi.org/10.1680/geot.1973.23.3.423.

Schor, H.J. and Gray, D.H. (2007), *Landforming: An Environmental Approach to Hillside Development, Mine Reclamation and Watershed Restoration*, Wiley, Hoboken, NJ.

Sokolovski, V.V. (1960), *Statics of Soil Media*, Butterworths Scientific Publications, London, UK.

Su, Z. and Shao, L. (2021), "A three-dimensional slope stability analysis method based on finite element method stress analysis", *Eng. Geol*., **280**(105910), 1-12. https://doi.org/10.1016/j.enggeo.2020.105910.

Taylor, D.W. (1937), "Stability of earth slopes", *J. Boston Soc. Civil Engineers*, **24**, 197-246.

Terzaghi, K. (1950), *Mechanisms of Landslides*, Geological Society of America, Berkeley Volume.

Terzi, N.U. and Selcuk, M.E. (2015), "Nonlinear dynamic behavior of Pamukcay earthfill dam", *Geomech. Eng*., **9**(1), 83-100. https://doi.org/10.12989/gae.2015.9.1.083.

Utili, S. and Nova, R. (2007), "On the optimal profile of a slope", *Soils Found.*, **47**(4), 717-729. https://doi.org/10.3208/sandf.47.717.

Vahedifard, F., Shahrokhabadi, S. and Leshchinsky, D. (2016), "Optimal profile for concave slopes under static and seismic conditions", *Can. Geotech. J.*, **53**(9), 1522-1532. https://doi.org/10.1139/cgj-2016-0057.

Veiskarami, M., Eslami, A. and Kumar, J. (2011), "End-bearing capacity of driven piles in sand using the stress characteristics method: analysis and implementation", *Can. Geotech. J.*, **48**(10), 1570-1586. https://doi.org/10.1139/t11-057.

Wasowski, J., Keefer, D.K. and Lee, C.T. (2011), "Toward the next generation of research on earthquake-induced landslides: current issues and future challenges", *Eng. Geol*., **122**(1-2), 1-8. https://doi.org/10.1016/j.enggeo.2011.06.001.

Yang, X., Zhai, E., Wang, Y. and Hu, Z. (2018), "A comparative study of pseudo-static slope stability analysis using different design codes", *Water Sci. Eng.*, **11**(4), 310-317. https://doi.org/10.1016/j.wse.2018.12.003.

Yuan, R., Deng, Q., Cunningham, D., Han, Z., Zhang, D. and Zhang, B. (2016), "Newmark displacement model for landslides induced by the 2013 Ms 7.0 Lushan earthquake, China", *Front. Earth Sci.*, **10**(4), 740-750. https://doi.org/10.1007/s11707-015-0547-y.

Zhou, X.P. and Cheng, H, (2014), "Stability analysis of three-dimensional seismic landslides using the rigorous limit equilibrium method", *Eng. Geol.*, **174**, 87-102. https://doi.org/10.1016/j.enggeo.2014.03.009.

JS